American Mineralogist, Volume 88, pages 1161–1164, 2003

LETTERS

Aluminum substitution in $MgSiO_3$ perovskite: Investigation of multiple mechanisms by ^{27}Al NMR

JONATHAN F. STEBBINS,[1,*] HIROSHI KOJITANI,[2] MASAKI AKAOGI,[2] AND ALEXANDRA NAVROTSKY[3]

[1]Department of Geological and Environmental Sciences, Stanford University, Stanford California 94305-2115, U.S.A.
[2]Department of Chemistry, Faculty of Science, Gakushuin University, 1-5-1 Mejiro, Toshima-ku, Tokyo 171-8588, Japan
[3]Thermochemistry Facility, Department of Chemical Engineering and Materials Science, University of California, One Shields Avenue, Davis, California 95616, U.S.A.

ABSTRACT

In the Earth's mantle, the mechanism(s) of solid solution of Al in $MgSiO_3$ perovskite strongly impacts its thermodynamic and transport properties. We present ^{27}Al NMR data for perovskite samples of nominal composition $Mg(Si_{0.9}Al_{0.1})O_{2.95}$, to test a mechanism by which Al^{3+} substitutes at the octahedral Si^{4+} sites, leaving a corresponding number of O-site vacancies. We find evidence for this process in a significantly greater peak area for Al at B (Si) sites vs. A (Mg) sites in the structure, and the possible identification of a small concentration of five-coordinated Al adjacent to such vacancies. However, substitution of Al^{3+} at the A sites remains significant. As in perovskite-type technological ceramics, O-atom vacancies may play an important role in enhancing ion mobility and the dissolution of water.

INTRODUCTION

The most common mineral in the Earth's lower mantle is $MgSiO_3$ with the perovskite structure, in which Si^{4+} occupies octahedral "B" sites ($^{[6]}Si$) and Mg^{2+} occupies central, eight- to twelve-coordinated "A" sites ($^{[8]}Mg$) (Knittle and Jeanloz 1987; Zhang and Weidner 1999). After FeO and possibly Fe_2O_3, the most abundant substituent in this phase is Al_2O_3, which comprises about 2 to 4 wt% of the entire mantle (Anderson 1989; Wood and Rubie 1996). Despite large effects on phase equilibria (Kesson et al. 1995; Wood and Rubie 1996; Weidner and Wang 1998; Kubo and Akaogi 2000), elastic (Zhang and Weidner 1999; Brodholt 2000) and electrical (Dobson and Brodholt 2000) properties, and their consequences for understanding the large-scale structure of the Earth, the mechanism(s) by which Al_2O_3 dissolves in $MgSiO_3$ perovskite are not fully understood.

Two types of solid solution have been proposed. A coupled substitution at both sites would maintain a 1:1 ratio of Mg/Si, with the composition remaining on the $MgSiO_3$-Al_2O_3 binary:

$$Mg^{2+}_A + Si^{4+}_B \leftrightarrow Al^{3+}_A + Al^{3+}_B \quad (1)$$

In contrast, Al^{3+} could substitute at the B site, leaving O-atom vacancies in the structure and producing compositions on the $MgSiO_3$-$MgAlO_{2.5}$ join:

$$Si^{4+}_B + 1/2O^{2-} \leftrightarrow Al^{3+}_B + 1/2V^0_O \quad (2)$$

O-atom vacancy substitutions are well-known in perovskite-structured oxides, for example the well-studied system $CaTiO_3$–$CaFeO_{2.5}$ (Becerro et al. 1999; McCammon et al. 2000). Such materials have important technological applications, especially when the resulting oxide ion mobility provides anionic conductivity in sensors and fuel cell electrolytes (Navrotsky 1999; Kim and Grey 2002; Stebbins 2002). It has been suggested that the second mechanism may play an important role in the lower mantle, which is likely to contain an MgO-rich oxide phase (ferropericlase) as well as perovskite, favoring a ratio of Mg/Si > 1 in the latter (Navrotsky 1999; Brodholt 2000). O-atom vacancies are particularly interesting as they may be a "sink" for hydroxyl groups and hence water in the earth (Navrotsky 1999; Murakami, et al. 2002) and may have large effects on diffusivity, conductivity, strength, and creep rate of the mantle. Stoichiometric $MgSiO_3$ perovskite, in contrast, apparently can accommodate very little OH in its structure (Bolfan-Casanova et al. 2000). As yet, however, there is no clear structural (as opposed to compositional) evidence for O-atom vacancies in $MgSiO_3$-based perovskites.

Recent spectroscopic studies of Al-substituted perovskite have concentrated on the stoichiometric join, $MgSiO_3$-Al_2O_3. X-ray absorption spectroscopy suggested that significant substitution occurs at both sites (Andrault et al. 1998). A high-field, high-resolution ^{27}Al NMR study of similar material revealed Al at two distinct types of sites, with roughly equal populations, favoring the domination by the coupled substitution in at least this composition (Stebbins et al. 2001). One site showed the symmetrical octahedral geometry expected for the defect-free B site; the other was more distorted and disordered, with six or higher coordination, suggesting a partially collapsed

* E-mail: Stebbins@pangea.stanford.edu

A site. Even in these materials, however, the occasional presence of small amounts of stishovite (SiO_2) has suggested some deviation from this ideal composition. Theoretical calculations based on a "brownmillerite" structure ($MgAlO_{2.5}$, with 50% $^{[4]}$Al and 50% $^{[6]}$Al) for the O-atom vacancy end-member favored reaction (2) at low pressure and (1) at high pressure (Richmond and Brodholt 1998; Brodholt 2000); first-principles, density-functional theory calculations on larger unit cells with lower and more realistic Al contents suggested that reaction (1) may be slightly more enthalpically stable (Yamamoto et al. 2003). This conclusion was also suggested by recent solution calorimetric studies (Navrotsky et al. submitted), which pointed out, however, that the difference in enthalpies is not large and that both mechanisms could be stabilized at high temperature by the configurational entropy resulting from disorder of cations and/or vacancies. The latter study also demonstrated that in systems with excess MgO, it is possible to form perovskites with non-stoichiometric compositions close to $Mg(Si_{0.9}Al_{0.1})O_{2.95}$, implying that O-atom vacancies are indeed present. Here, we apply ^{27}Al NMR to elucidate the mechanism or mechanisms at the atomic scale.

Experimental methods

Perovskite with a nominal composition of $MgSi_{0.9}Al_{0.1}O_{2.95}$ was synthesized with techniques similar to those recently described (Navrotsky et al. 2003) from reagent-grade oxides, including 0.1 wt% cobalt oxide to speed spin-lattice relaxation. After mixing and drying at 1000 °C, five samples were loaded into rhenium tubes and heated at 1600 °C and 27 GPa in a "6–8" multianvil apparatus (Kawai type) (Kubo and Akaogi 2000) for 3 h. Each sample was examined intact (uncrushed) by microfocus X-ray diffraction using a Rigaku RINT-2500V diffractometer (Kubo and Akaogi 2000); only the perovskite phase was observed. After the NMR experiments, extensive electron microprobe analyses were done on two samples. Although the small grain size and damage by the electron beam reduced analytical precision, it is clear that two types of perovskite grains were present in each of the two samples, with average compositions of $(Mg_{0.96}Al_{0.04})(Si_{0.96}Al_{0.04})O_{3.0}$ and $(Mg_{0.97}Al_{0.03})(Si_{0.94}Al_{0.06})O_{2.98}$ respectively, where twice the standard deviation of the mean for the cation fractions is about 0.005. Some points with excess Mg were noted, indicating the presence of a minor amount of MgO; no points attributable to corundum (Al_2O_3) were observed. The origin of this heterogeneity is uncertain but could be related to thermal gradients during synthesis.

To enhance sensitivity for the small samples produced by the high-pressure experiments, to produce relatively narrow, quantifiable peaks for Al sites with large quadrupolar coupling constants, and to determine second-order quadrupolar shifts from the variation in peak position with field, ^{27}Al MAS NMR spectra were collected at relatively high magnetic fields with Varian Unity/Inova 600 (14.1 Tesla) and 800 (18.8 T) spectrometers. Varian/Chemagnetics "T3" probes with 3.2 mm ZrO_2 rotors and spinning rates of 18 kHz were used, along with single pulse acquisition with short pulses (0.2 µs, 30° estimated rf tip angle for the solid). Frequencies (156.3 and 208.4 MHz) were referenced to external 0.1 M $Al(NO_3)_3$. Instrumental deadtime was about 15–20 µs; a significant rotor background signal was subtracted. Perovskite samples were loaded as five intact pellets (not crushed) totaling about 1.5 mg. Spectra with delay times ranging from 0.05 to 10 s were collected. Short delays gave the best signal-to-noise ratios and were used to simulate line shapes. In comparison to a previous study (Stebbins et al. 2001), the B-site peak relaxed more slowly than the A-site peak, requiring longer delay spectra to estimate true relative intensities. Simulations of peak shapes and positions were matched by eye to the experimental spectra at both fields, using the Varian "STARS" software. Significant Gaussian peak broadening was required to match observed peak shapes. After simulating peaks "A" and "C" (see below), the area of the non-Gaussian peak "B" was determined by subtraction. Uncertainties in simulations were estimated from sensitivity of calculated peak shapes to variations in parameters. To check for accurate quantification of the NMR peak areas, a mechanical mixture of AlN, sodalite ($Na_8Al_6Si_6O_{24}Cl_2$), and kyanite (Al_2SiO_5) was made and run under conditions identical to the Al-perovskite. The first two phases have C_Q values among the lowest known for ^{27}Al (<1 MHz), while the latter has three sites with C_Q from 3.7 to 10 MHz. Measured peak areas agreed with ideal values within about 1% absolute.

Results and discussion

The major features of the ^{27}Al NMR spectra (Fig. 1) are similar to those reported for perovskites of approximate composition $(Mg_{0.95}Al_{0.05})(Si_{0.95}Al_{0.05})O_3$ (Stebbins et al. 2001). The derived NMR parameters of the most intense, narrow peak are the same within error; the mean quadrupolar coupling constant (C_Q) and isotropic chemical shift (δ_{iso}) for the broader peak are somewhat less than in the previous report, possibly due to some difference in ordering state resulting from different starting materials (compositions and glassy vs. crystalline) and run conditions. However, there are two major differences between the results from the "stoichiometric" vs. the "Si-deficient" samples. In the latter, the relative intensity of the B-site peak is consid-

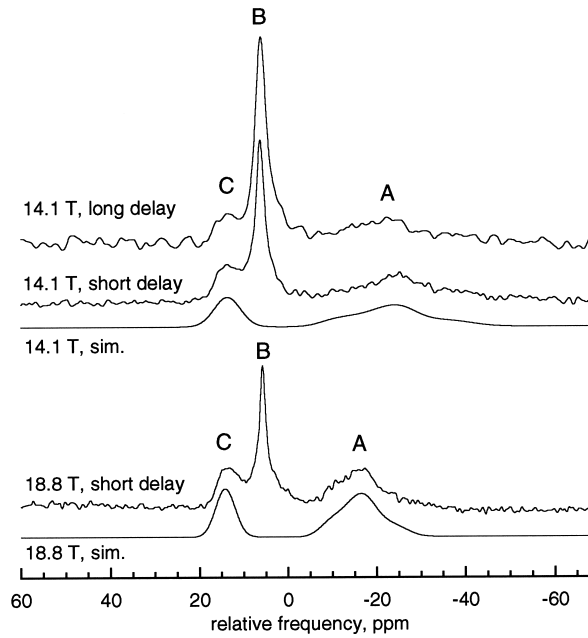

Figure 1. ^{27}Al MAS spectra for perovskite of nominal composition $MgSi_{0.9}Al_{0.1}O_{2.95}$, collected at fields shown. "A" indicates the A-site peak; "B" indicates the B-site peak; peak "C" may be due to five-coordinated Al at B sites adjacent to O-atom vacancies (see text). At 14.1 T, the spectrum with the "long" delay between rf pulses is the sum of spectra for delays of 4 and 10 s (which were identical in shape); the "short" delay data were acquired with a delay of 0.05 s. The latter was processed with less apodization than the former, resulting in a somewhat narrower "B" peak. At 18.8 T, a pulse delay of 0.20 s was used for the data shown. Simulations of the "A" and "C" peaks were done with the same parameters at both fields. For A, $\delta_{iso} = -7 \pm 2$ ppm, $C_Q = 7.5 \pm 0.5$ MHz; for C, $\delta_{iso} = 15 \pm 1$ ppm, $C_Q = 2.0 \pm 0.5$ MHz; for both, η was chosen as 0.75 but is poorly constrained. Quadrupolar peak shapes were convolved with a Gaussian to roughly simulate the effects of disorder and to produce the observed peak shapes. The position of peak "B" is consistent with $\delta_{iso} = 5.8 \pm 0.3$ ppm and $C_Q \approx 1$ MHz (Stebbins et al. 2001).

erably greater than that of the A-site peak, while in the former both peaks have roughly the same area. The spectra of the Si-deficient samples also have a third prominent peak ("C") centered at about +14 ppm (Fig. 1); this feature is present at most as a small, unresolved shoulder in the spectrum for one of the "stoichiometric" samples. The relative areas (± roughly 4% absolute) for the three peaks in fully relaxed spectra are C: 14%, B: 59%, and A: 27%, which represent the fractions of the total Al in the combined samples at each of the three site types, when integrated over all of the grains (possibly of somewhat varying compositions).

The estimated δ_{iso} and C_Q of peak "C" (15 ppm and 2.0 MHz) are similar to published data for corundum (α-Al_2O_3) of 16 ppm and 2.39 MHz (Stebbins 1995), but those values do not reproduce the effect of field on the peak position as well. Given the total fraction of the alumina component in the sample and the relative area of peak "C", only about 0.7 wt% of corundum would be needed. However, if corundum were present in particles greater than about 1 μm in diameter, even this small amount should have been detected by the EMPA mapping; the high temperature annealing time should probably allow grain growth to at least this size. A possible test of whether the breadth of this peak is due to disorder at a site in perovskite (expected to give a width constant in ppm) or to residual homonuclear (Al-Al) dipolar broadening in corundum (expected to give a width constant in Hz) is not definitive given the signal-to-noise ratio, peak overlap, and the relatively small ratio of the two fields used.

The large ratio of B-site to A-site intensities (≈2.2) implies that O-atom vacancies should be present in the structure of a significant fraction of the perovskite grains. However, it is unlikely that the Al^{3+} cations giving rise to the relatively narrow, main, B-site peak ($C_Q \approx 1$ MHz, Stebbins et al. 2001) are adjacent to O-atom vacancies, as the chemical shift is far outside the known range for five-coordinated Al and a greater local distortion from cubic symmetry would be expected. Rather, we suggest that Al sites producing the small "C" peak may represent such defects. Although the chemical shift of 15 ppm is also outside the "normal" expected range for $^{[5]}$Al in silicates and oxides of about 30 to 40 ppm (Stebbins 1995), it is close to that for trigonal bipyramidal $^{[5]}$Al sites best known in $SrAl_{12}O_{19}$, where δ_{iso} has been accurately measured as 18.0 ppm ($C_Q = 2.1$ ppm) (Jansen et al. 1998). The likely cause for this extreme value of δ_{iso} is the unusually long mean Al-O bond distance of 0.195 nm for the $^{[5]}$Al sites (Kimura et al. 1990), compared to more "typical" values for $^{[5]}$Al in a mineral such as andalusite (Al_2SiO_5, 0.184 nm, Winter and Ghose 1979; δ_{iso} = 35 ppm, Stebbins 1995). Unusually long bond distances might occur at defect $^{[5]}$Al sites in $MgSiO_3$ perovskite if the long-range structure does not allow Al-O bond distances in such defects to contract from typical octahedral to typical five-coordinate values. If this assignment is correct, the relatively low intensity of the "C" peak suggests that O-atom vacancies are not strongly ordered next to Al at B sites; instead, a near-random substitution on the O-atom lattice is suggested, an assumption used recently in estimating the configurational entropy resulting from Al substitution (Navrotsky et al. 2003). If peak "C" does not represent $^{[5]}$Al, then the overall results are much more difficult to interpret. Alternatively, it is conceivable that the $^{[5]}$Al sites have extremely large C_Q values (>15 MHz?), broadening their NMR peak enough to be difficult to observe in such small samples even at 18.8 T.

The chemical shift for the A-site peak (–7 ppm) is at the extreme low end of values reported for $^{[6]}$Al in oxides and silicates (Stebbins 1995), and may represent Al with six or more O-atom neighbors and relatively long bond distances. O-atom vacancies could also reduce the average coordination number of Al^{3+} at A sites to less than the value of eight for Mg^{2+} in pure $MgSiO_3$ perovskite at ambient conditions. As for the "C" peak, simulation of the A-site peak required convolution of the quadrupolar line shape with a high degree of Gaussian broadening, indicating significant disorder introduced by variation in next-nearest neighbor cation and/or vacancy location. The B-site peak is also broader at the base than expected from its low C_Q, which again suggests some disorder.

The samples studied by NMR thus appear to contain Al^{3+} at the B sites, with both symmetrical six-coordinate and distorted, five-coordinate geometries, and in large, central A sites. This finding is consistent with electron microprobe data indicating the presence of grains both with stoichiometric Al substitution (Mg/Si ≈ 1) and with excess Al at the B sites (Mg/Si > 1). If, as we suggest, the locations of the O-atom vacancies in the latter type of material are not strongly correlated with those of the B sites containing Al^{3+}, then the $MgSiO_3$–$MgAlO_{2.5}$ binary (at least at low Al contents) resembles the well-studied $CaTiO_3$–$CaFeO_{2.5}$ system at low Fe^{3+} contents. At an Fe component fraction of 0.11 (prepared at 1320 °C), for example, Mössbauer spectra showed that 63% of the Fe^{3+} was at octahedral sites, with only 29% at pentahedral sites adjacent to one vacancy (McCammon et al. 2000) (8% of the Fe^{3+} was at tetrahedral sites adjacent to pairs of vacancies).

The quantitative application of these results for samples at ambient temperature and pressure to more complex phases under actual mantle conditions necessarily requires assumptions about lack of significant structural rearrangement during quench and depressurization; evidence for some unquenchable Al/Mg disorder at very high temperature in spinel ($MgAl_2O_4$) has been presented, for example (Wood et al. 1986). However, our data do indicate that both proposed mechanisms of substitution of Al into $MgSiO_3$ perovskite are likely to be important in a mantle with Mg/Si > 1. Regardless of the detailed contributions from the two processes, the NMR results rule out two proposed models. An ideal, ordered "brownmillerite" structure is excluded by the observed absence of $^{[4]}$Al; an ordered model of pairs of B-site Al^{3+} cations adjacent to each O-atom vacancy is not consistent with the relatively low concentration of $^{[5]}$Al. The O-atom vacancies that are present, and which are apparently mainly disordered, will need to be considered not only in calculations of thermodynamic mixing properties (and hence phase equilibria), but in models of elastic constants and transport phenomena as well. Our initial constraints on the extent of disorder among cations at A and B sites, and of O-atom vacancies, will lead to more accurate estimation of the configurational entropy, which is in turn critical to extending thermodynamic calculations to the high temperatures of the lower mantle. The interactions among Al^{3+} and other substitu-

ents, notably Fe^{2+} and Fe^{3+} (McCammon 1997) will need to be considered for real mantle compositions; spectroscopic results for more homogeneous samples are of course desirable. Finally, a defect-rich perovskite may serve as a significant host for water in the lower mantle, with important implications for the thermal and degassing history of the earth (Navrotsky 1999; Murakami et al. 2002).

ACKNOWLEDGMENTS

We thank D. Rice and E. Williams for access to and assistance with 800 the MHz spectrometer at Varian Inc. in Palo Alto, and T. Sugawara and E. Takahashi for help with the EPMA work. This work was supported by NSF grant EAR 0104926 to J. Stebbins and grants in aid for scientific research from JSPS.

REFERENCES CITED

Anderson, D.L. (1989) Theory of the Earth, 366 p. Blackwell, Oxford, U.K.

Andrault, D., Neuville, D.R., Flank, A.M., and Wang, Y. (1998) Cation sites in Al-rich $MgSiO_3$ perovskites. American Mineralogist, 83, 1045–1053.

Becerro, A.I., McCammon, C., Langenhorst, F., Seifert, F., and Angel, R. (1999) Oxygen vacancy ordering in $CaTiO_3$-$CaFeO_{2.5}$ perovskites: from isolated defects to infinite sheets. Phase Transitions, 69, 133–146.

Bolfan-Casanova, N., Keppler, H., and Rubie, D.C. (2000) Water partitioning between nominally anhydrous minerals in the MgO-SiO_2-H_2O system up to 24 GPa: implications for the distribution of water in the earth's mantle. Earth and Planetary Science Letters, 182, 209–221.

Brodholt, J.P. (2000) Pressure-induced changes in the compression mechanism of aluminous perovskite in the Earth's mantle. Nature, 407, 620–622.

Dobson, D.P. and Brodholt, J.P. (2000) The electrical conductivity and thermal profile of the earth's mid-mantle. Geophysical Research Letters, 27, 2325–2328.

Jansen, S.R., Hintzen, H.T., Metselaar, R., de Haan, J.W., van de Ven, L.J.M., Kentgens, A.P.M., and Nachtegaal, G.H. (1998) Multiple quantum ^{27}Al magic-angle-spinning nuclear magnetic resonance spectroscopic study of $SrAl_{12}O_{19}$: identification of a ^{27}Al resonance from a well-defined AlO_5 site. Journal of Physical Chemistry B, 102, 5969–5976.

Kesson, S.E., FitzGerald, J.D., Shelley, J.M.G., and Withers, R.L. (1995) Phase relations, structure and crystal chemistry of some aluminous silicate perovskites. Earth and Planetary Science Letters, 134, 187–201.

Kim, N. and Grey, C. (2002) Probing oxygen motion in disordered anionic conductors with ^{17}O and ^{55}V NMR spectroscopy. Science, 297, 1317–1320.

Kimura, K., Ohgaki, M., Tanaka, K., Morikawa, H., and Marumo, F. (1990) Study of the bipyramidal site in magnetoplumbite compounds, $SrM_{12}O_{19}$ (M=Al, Fe, Ga). Journal of Solid State Chemistry, 87, 186–194.

Knittle, E. and Jeanloz, R. (1987) Synthesis and equation of state of (Mg,Fe)SiO_3 perovskite to over 100 GPa. Science, 235, 669–670.

Kubo, A. and Akaogi, M. (2000) Post-garnet transitions in the system $Mg_4Si_4O_{12}$-$Mg_3Al_2Si_3O_{12}$ up to 28 GPa: phase relations of garnet, ilmenite and perovskite. Physics of Earth and Planetary Interiors, 121, 85–102.

McCammon, C. (1997) Perovskite as a possible sink for ferric iron in the lower mantle. Nature, 387, 694–696.

McCammon, C.A., Beccerro, A.I., Langenhorst, F., Angel, R.J., Marion, S., and Seifert, F. (2000) Short-range ordering of oxygen vacancies in $CaFe_xTi_{1-x}O_{3-x/2}$ perovskites ($0<x<0.4$). Journal of Physics: Condensed Matter, 12, 2969–2984.

Murakami, M., Hirose, K., Yurimoto, H., Nakashima, S., and Takafuji, N. (2002) Water in the earth's lower mantle. Science, 295, 1885–1887.

Navrotsky, A. (1999) A lesson from ceramics. Science, 284, 1788–1789.

Navrotsky, A., Schoenitz, M., Kojitani, H., Xu, H., Zhang, J., Weidner, D., Jeanloz, R. (2003) Aluminum in magnesium silicate perovskite: formation, structure, and energetics of magnesium-rich defect solid solutions. Journal of Geophysical Research, in press.

Richmond, N.C. and Brodholt, J.P. (1998) Calculated role of aluminum in the incorporation of ferric iron into magnesium silicate perovskite. American Mineralogist, 83, 947–951.

Stebbins, J.F. (1995) Nuclear magnetic resonance spectroscopy of silicates and oxides in geochemistry and geophysics. In T. J. Ahrens, Eds., Handbook of Physical Constants, p. 303–332. American Geophysical Union, Washington D.C.

——— (2002) Dynamics in Ceramics. Science, 297, 1285–1286.

Stebbins, J.F., Kroeker, S., and Andrault, D. (2001) The mechanism of solution of aluminum oxide in mantle perovskite ($MgSiO_3$). Geophysical Research Letters, 28, 615–618.

Weidner, D.J. and Wang, Y. (1998) Chemical- and Clapeyron-induced buoyancy at the 660 km discontinuity. Journal of Geophysical Research, 103, 7431–7441.

Winter, J.K. and Ghose, S. (1979) Thermal expansion and high-temperature crystal chemistry of the Al_2SiO_5 polymorphs. American Mineralogist, 64, 573–586.

Wood, B.J. and Rubie, D.C. (1996) The effect of alumina on phase transformations at the 660-kilometer discontinuityfrom Fe-Mg partitioning experiments. Science, 273, 1522–1524.

Wood, B.J., Kirkpatrick, R.J., and Montez, B. (1986) Order-disorder phenomena in $MgAl_2O_4$ spinel. American Mineralogist, 71, 999–1006.

Yamamoto, T.,Yuen, D.A., Ebisuzuki, T. (2003) Substitution mechanism of Al ions in $MgSiO_3$ perovskite under high pressure conditions from first-principles calculations. Earth and Planetary Science Letters, 206, 617–625.

Zhang, J. and Weidner, D.J. (1999) Thermal equation of state of aluminum-enriched silicate perovskite. Science, 284, 782–784.

MANUSCRIPT RECEIVED OCTOBER 19, 2002
MANUSCRIPT ACCEPTED JANUARY 13, 2003
MANUSCRIPT HANDLED BY LEE GROAT